



Determining the GaSb/GaAs-(2 × 8) reconstruction

Jessica E. Bickel^a, Normand A. Modine^b, Joanna Mirecki Millunchick^{a,*}

^a Department of Materials Science and Engineering, The University of Michigan, Ann Arbor, MI 48109, United States

^b Center for Integrated Nanotechnologies, Sandia National Laboratories, Albuquerque, NM 87185, United States

ARTICLE INFO

Article history:

Received 6 April 2009

Accepted for publication 28 July 2009

Available online 7 August 2009

Keywords:

Surface relaxation and reconstruction

Density functional calculations

Molecular beam epitaxy

ABSTRACT

Highly strained thin layers of GaSb/GaAs possess a (2 × 4) reconstruction at low Sb overpressures, and a (2 × 8) reconstruction at high Sb overpressures. While the atomic details of the Sb/GaAs-(2 × 4) are well known, the details of the (2 × 8) are not understood. In this paper, we use density functional theory to analyze possible (2 × 8) structures. Comparing scanning tunneling microscope images from both simulation and experiment and examining the relative energies of possible (2 × 8) structures, we show the $\alpha(2 \times 8)$ and $\beta(2 \times 8)$ are the thermodynamically stable surface reconstructions for high Sb content films strained to the GaAs lattice parameter. The α and $\beta(2 \times 8)$ reconstructions are related to the GaAs- $\alpha 2(2 \times 4)$ and GaAs- $\beta 2(2 \times 4)$ through the addition of 2 cations and 8 anions into the trench between adjacent (2 × 4) unit cells.

© 2009 Elsevier B.V. All rights reserved.

1. Introduction

Surface reconstructions are present in a wide variety of materials systems and are known to impact the system in a variety of ways including interface development [1], catalysis [2], oxide growth [3], atomic bulk ordering [1], epitaxial film growth [4], and magnetic domain orientation [5]. Surface reconstructions form in order to minimize the energy of a cleaved surface resulting from a high number of dangling bonds. They consist of long range 2D periodicities whose structure is governed by the competing effects of (1) local chemistry, which drives the formation of new covalent bonds to minimize energy, (2) long range electrostatics, which forces the surface to remain charge neutral according to the electron counting rule (ECR) [6] by requiring filled anion dangling bonds and empty cation dangling bonds, and (3) local displacement strain, which increases the energy as the new bonds require atoms to be displaced from their bulk atomic positions. These three competing interactions are the fundamental physical factors impacting binary compound semiconductor surfaces and have been used to predict the surface reconstructions as a function of chemical potential [7,8]. However, in the case where a film is alloyed or is lattice mismatched relative to the substrate, additional phenomena, including lattice mismatch strain and localized atomic size mismatch strain, also influence the surface stability. Lattice mismatch strain may induce the coexistence of multiple surface reconstructions with the surface morphology dictating the surface reconstruction in order to relieve the strain [9–11], and atomic size

mismatch strain may drive surface ordering in alloyed films [12,13].

Lattice mismatched films such as GaSb/GaAs are used in lasers, detectors, solar cells, and transistors [14]. The growth of these films is limited to a few monolayers, as the critical thickness for 3D islands is approximately 3 monolayers (ML). Thicker films can be grown, but their usefulness is limited by the introduction of threading dislocations that propagate through the film and act as non-radiative recombination centers. The 2D–3D transition is determined by the strain energy due to lattice mismatch and the difference in surface energies of GaAs and GaSb. These surface energies are determined by the film chemistries, surface reconstruction, and surface strain. Recent work by Huffaker et al. demonstrated that the initial surface conditions have a dramatic effect on the final defect structure of highly lattice mismatched GaSb/GaAs films [15–17]. These results show that changing the initial surface reconstruction from a GaAs-(2 × 4) to a GaSb-(2 × 8) greatly impacts the defect structure of the resulting films which controls the use of these films in devices that require defect free active zones, as well as impacting the size, shape, and density of grown quantum dots, which might be used to affect self-assembly. This clearly illustrates the importance of having a detailed understanding of the surface structure of thin films of GaSb on GaAs and the growth parameters necessary to obtain different surface structures in this system.

Several researchers have examined Sb capped GaAs, which is a reasonable system to examine interfacial formation between GaAs and GaSb. In Sb/GaAs, anion exchange results in very thin films of GaSb/GaAs. In this system, researchers found that the most common reconstructions are the (2 × 4) reconstruction which is stable

* Corresponding author.

E-mail address: joannamm@umich.edu (J.M. Millunchick).

under moderate Sb pressures or higher growth temperatures [18–21], and the (2×8) reconstruction which is stable under high Sb pressures or lower growth temperatures [22,23]. While the structure of the (2×4) is known [23], that of the (2×8) remains uncertain. In this paper, the structures of several proposed (2×8) reconstructions are examined and compared to experimental results. The stability of these models are examined computationally as a function of lattice mismatch strain for these thin, coherently strained GaSb/GaAs films.

2. Experimental results and discussion

The (2×8) reconstruction appears for very thin layers of GaSb on GaAs grown under Sb rich conditions. It is typically obtained by saturating a GaAs surface with Sb [22–24]. In typical experiments, the GaAs surface is exposed to a high flux of Sb inside a molecular beam epitaxy (MBE) chamber so that the reflection high energy electron diffraction (RHEED) pattern changes from the (2×4) reconstruction, to an incommensurate (1×3) pattern (not reported by all groups), then to a (2×8) reconstruction (for further experimental details please see [24]). The Sb replaces the As on the surface through a process called anion exchange [25], resulting in a GaSb film a few monolayers thick. Beyond this thickness, the films are saturated and little to no additional Sb incorporates into the surface [24]. Cooling this surface in the absence of an Sb overpressure, the reconstruction quickly reverts to (2×4) according to RHEED, though STM shows that the surface actually contains both $\alpha(2 \times 4)$ and $\alpha(4 \times 3)$ surface reconstruction domains [24]. Cooling this surface under an Sb overpressure results in a stabilization of the (2×8) reconstruction. The reversion to the mixed surface reconstruction under no Sb flux suggests desorption of Sb from the (2×8) reconstructed surface because the Group V species are quite volatile. These observations are consistent with the notion that the (2×8) reconstruction contains excess Sb [22–24].

Fig. 1 shows an STM image of a (2×8) reconstruction of Sb/GaAs grown by molecular beam epitaxy using solid source Ga and valved-cracker As and Sb sources. The GaAs surface was prepared as described previously [24]. The film was grown at $T \sim 525^\circ\text{C}$ and $R_{\text{Sb}} = 0.36\text{ML/s}$. The Sb_2 flux was then reduced to $R_{\text{Sb}} = 0.15\text{ML/s}$ and the sample was rapidly cooled to $T = 200^\circ\text{C}$ and transferred *in vacuo* to be characterized using STM. The (2×8) reconstruction consists of straight rows of atoms along the $[1\bar{1}0]$ direction. These rows are spaced regularly along the $[1\bar{1}0]$ at 32Å , as can be seen in Fig. 1c, corresponding to a periodicity of eight times the bulk in-plane lattice parameter a_0 , where a_0

is between the GaAs and GaSb lattice parameters. A linescan across the reconstruction rows shows very little structural detail, only an approximately sinusoidal variation in apparent height. Further structural definition was not possible given the difficulty in keeping a stable image at the higher voltages required for these GaSb samples. There is a slight amount of disorder on the surface where the rows diverge and recombine, which is likely due to the fact that the sample was quenched without additional annealing. Similar disorder appears in the STM images by Whitman et al. [22] though not in those by Laukannen et al. [23]. This suggests the disorder may be thermally unstable and anneal out under long Sb exposures.

3. Computational results and discussion

In this paper, we examine four possible (2×8) structures. Each of the structures obeys the ECR and terminates in a double anion layer, as suggested by experimental observations. The first structure was initially proposed for the InSb- (2×8) reconstruction [26], and is referred to here as the $\alpha(2 \times 8)$ (Fig. 2a). This structure consists of a backbone of Sb dimers along the $[1\bar{1}0]$ (two dimers per unit cell) in the topmost Sb layer. This layer sits atop a second Sb layer, which has an additional four anion dimers along the $[1\bar{1}0]$ which orient parallel to the $[1\bar{1}0]$. A final anion dimer sits in the trench between adjacent unit cells. We term this structure the $\alpha(2 \times 8)$ because it contains a single unit cell of the $\alpha(2 \times 4)$ reconstruction common to III-As systems (outlined in Fig. 2a-left). The $\alpha(2 \times 8)$ reconstruction may be easily constructed from a base structure of two $\alpha(2 \times 4)$ cells by adding 2 Ga and 8 Sb atoms above the central trench dimer. A simulated filled state STM image is shown in the center of Fig. 2a, and was generated using the method proposed by Tersoff et al. [27]. A single (2×8) unit cell is outlined in the simulated STM image. This STM image shows the almost constant value of the electron density along the anion backbone along the $[1\bar{1}0]$ and a periodic increase and decrease along the $[1\bar{1}0]$. This variation also appears in a linescan in the $[1\bar{1}0]$, determined from averaging the z-height at all $[1\bar{1}0]$ positions within the unit cell (Fig. 2a-right). The original data is shown in the dotted line, and the result is smoothed using a Steinman function and applying a geometric weighting of the nearest 10% of data points to get the solid line. This smoothed function more accurately simulates a rounded STM tip and results in an almost sinusoidal change in apparent height. The second structure, the $\beta(2 \times 8)$, (Fig. 2b) is similar, except that it is built from the III-As $\beta(2 \times 4)$ reconstruction that contains two Sb surface dimers (out-

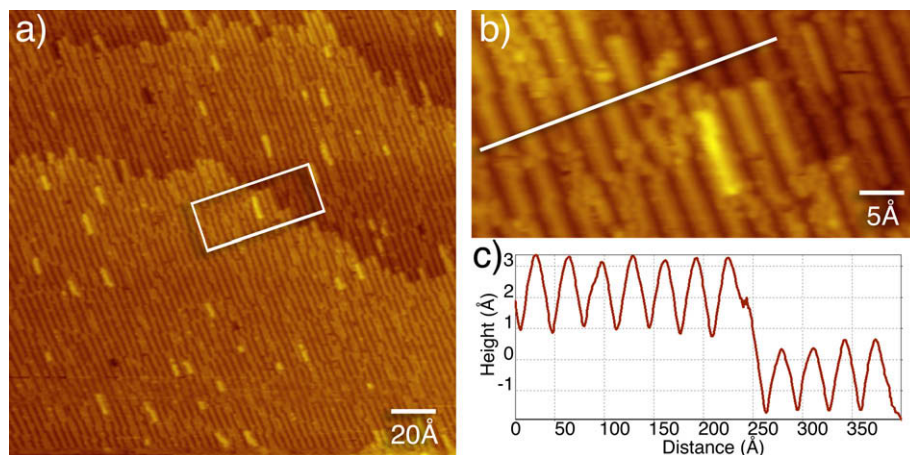


Fig. 1. (a) STM image ($V = -4.07\text{ V}$, $I = 100\text{ pA}$) of 2.0ML Sb/GaAs cooled under Sb flux to form the (2×8) reconstruction. (b) High resolution portion of the image in (a). (c) A line scan across the line indicated in (b). (For interpretation of the references to colors in this figure, the reader is referred to the web version of this paper.)

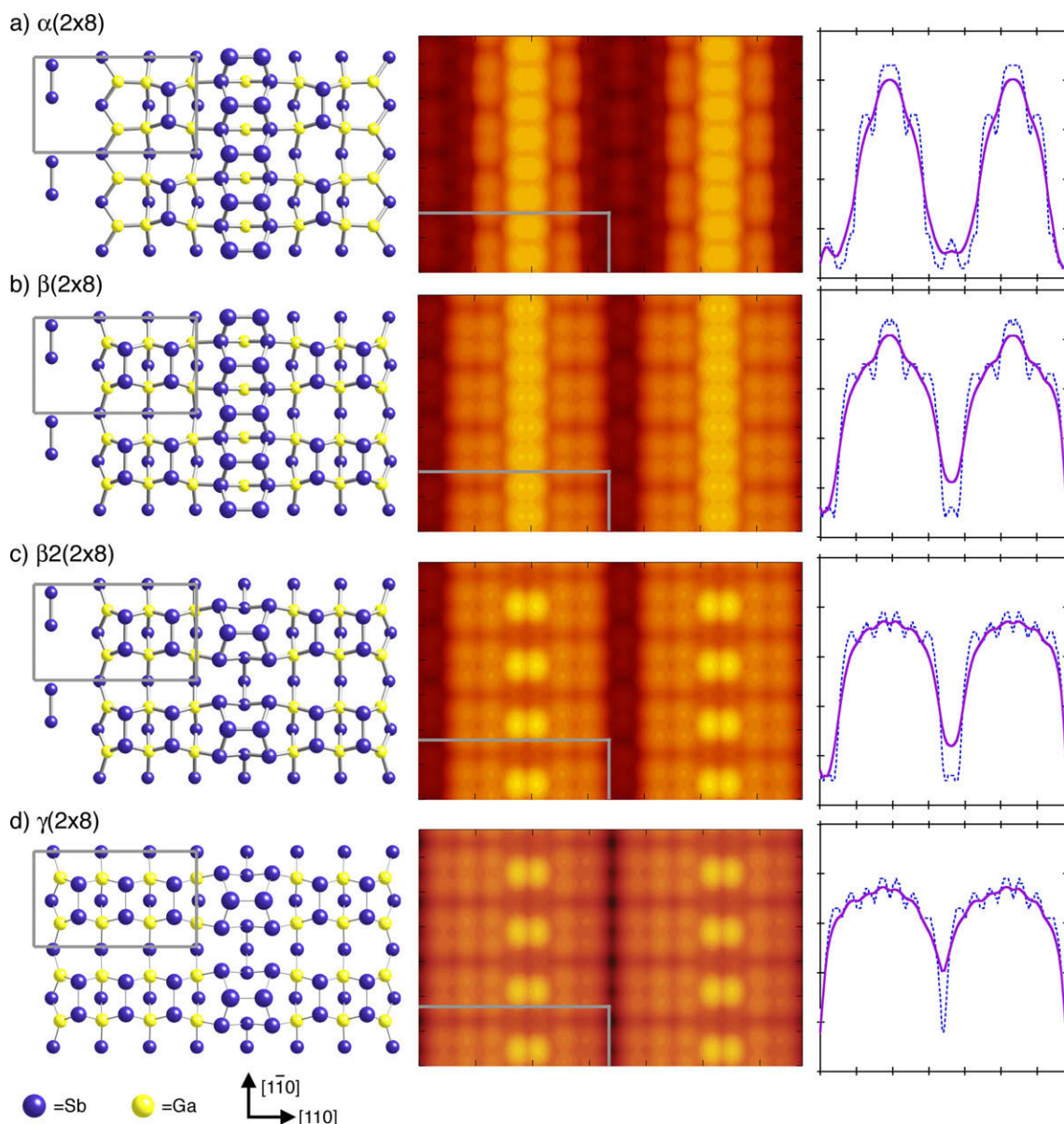


Fig. 2. Proposed structures for the GaSb/GaSb-(2×8) reconstruction. (a) $\alpha(2 \times 8)$, (b) $\beta(2 \times 8)$, (c) $\beta_2(2 \times 8)$, and (d) $\gamma(2 \times 8)$. On the left are the atomic structures (note: some atoms removed for clarity). In the middle are simulated filled state (negative bias) STM images (ticks = 10 Å). On the right are line scans of the simulated STM images with the original data (dotted line) and a smoothed line (solid line) calculated using a Steinman function and applying a geometric weighting of the nearest 10% of data points (x -ticks = 10 Å and y -ticks = 1 Å). (For interpretation of the references to colors in this figure, the reader is referred to the web version of this paper.)

lined in Fig. 2b-left) and exhibits a similar simulated STM image and line scan. The addition of an extra Sb surface dimer to the horizontal results in wider rows along the $[1\bar{1}0]$ changing the line scan shape to a cycloid. The third structure was proposed by Laukkanen et al. [23] as a possible structure for the GaSb-(2×8) reconstruction. Because this structure also contains the $\beta_2(2 \times 4)$ unit cell as a basis structure, we term it the $\beta_2(2 \times 8)$ reconstruction. The $\beta_2(2 \times 8)$ only has a single Sb dimer in the topmost surface layer, which requires the introduction of Sb atoms into anti-sites in the topmost cation layer to maintain charge neutrality. The simulated STM image differs from that of the $\beta(2 \times 8)$ in that it shows a periodic change in intensity along the $[1\bar{1}0]$ due to the presence of the single anion dimer per unit cell. The $[1\bar{1}0]$ line scan is very similar to that in Fig. 2b, but lower in amplitude due to averaging over the periodically missing anion dimer. The final structure is a modification of that proposed by Whitman et al. [22] as a possible structure for the GaSb-(2×8) reconstruction

and is shown in Fig. 2d. This structure, herein termed as the $\gamma(2 \times 8)$, resembles that of the $\beta_2(2 \times 8)$, containing the same missing dimer along the $[1\bar{1}0]$ that requires two Sb anti-sites. This structure does not have a trench dimer; instead, the trench is filled with an additional pair of Ga atoms and As dimer. The results is another III-As unit cell on the left of the Sb dimer chain $[1\bar{1}0]$ backbone, the $\beta(2 \times 4)$ unit cell [28] (outlined Fig. 2d-left) which is a three dimer structure, and a two dimer structure on the right side of the reconstruction. This configuration admits the possibility for disorder within the structure as the three dimer and two dimer structures can change sides in adjacent until cells resulting in the topmost Sb dimer backbone shifting positions between adjacent unit cells. The simulated STM of the $\gamma(2 \times 8)$ structure is similar to that of the $\gamma_2(2 \times 8)$ without a gap for the trench dimer, and the resulting linescan is shallow in depth between adjacent unit cells due to the lack of the trench and takes on a shallow centroid shape.

Qualitative similarities between the experimental and simulated STM images suggest that that $\alpha(2 \times 8)$ reconstruction is a promising candidate for the atomic structure of the experimentally obtained (2×8) reconstruction. Both the $\alpha(2 \times 8)$ and $\beta(2 \times 8)$ structures exhibit straight rows of intensity along the $[110]$, in agreement with the straight row of intensity seen in Fig. 1a, along the dimer backbone. However, examination of the linescan in Fig. 1c shows a very sinusoidal character with almost even widths of the peak and valley. The $\beta(2 \times 8)$ reconstruction shows a broader peak with a narrow valley, while the $\alpha(2 \times 8)$ shows a linescan which closely resembles a sinusoid, suggesting the $\alpha(2 \times 8)$ structurally agrees with experimental results.

The relative stabilities of these four possible (2×8) structures were examined using Density Functional Theory (DFT). Calculations were performed as described previously [9] examining the surface reconstructions imposed upon a periodically repeating slab structure. k -point meshes were 6×3 , 3×4 , 3×3 , and 6×2 for the 2×4 , 4×3 , 4×4 , and 2×8 slabs, respectively. The surface energies of the four potential (2×8) reconstructions are plotted against those of other common anion-rich surface reconstructions of pure, relaxed GaAs, including the (2×4) family of reconstructions, and pure, relaxed GaSb, which exhibits the (4×3) family of reconstructions. GaSb slabs were used in all energy calculations because the surface is assumed to be pure GaSb due to the tendency of Sb to surface segregate [1]. The results are shown in Fig. 3a–c for pure GaSb slabs relaxed at the GaSb, InP, and GaAs lattice parameters respectively. The grand canonical surface free energies were determined by relaxing each structure, then relating the surface energy to the surface stoichiometry and Sb chemical potential according to the method described by Wixom et al. [29]. The resulting energy values are plotted along the y -axis in eV vs. the chemical potential of Sb relative to that of bulk, rhombohedral Sb, $\mu_{\text{Sb}} - \mu_{\text{Sb(bulk)}}$ on the x -axis. The lowest curve at any given chemical potential is the thermodynamically stable reconstruction, with higher energy reconstructions energetically inaccessible. The x -axis boundaries are determined by the bulk energy of rhombohedral Sb and the calculated formation energy of GaSb, which is -0.3 eV per GaSb unit. This value is slightly smaller than experimentally reported values [30], however, the predicted stable reconstructions at the GaSb and GaAs lattice parameters agree qualitatively with the experimental results.

GaSb surface reconstructions were examined at three different lattice parameters in order to determine how stability changes as a function of strain. The three lattice parameters examined are: (1) GaSb, as a control state because the surface structure of GaSb at the GaSb lattice parameter is relatively well understood [31], (2) InP, an intermediate lattice parameter chosen to examine the stability of the surface reconstructions changes as a function of compressive strain, and (3) GaAs, as this is nominally the lattice parameter of the film in the experiments. Fig. 3a shows that for GaSb at the GaSb lattice parameter, the stable reconstructions with increasing μ_{Sb} are the $\alpha(4 \times 3)$, $\beta(4 \times 3)$ and $c(4 \times 4)$. The $\alpha(4 \times 3)$ and $\beta(4 \times 3)$ reconstructions are experimentally observed and are generally accepted to be the stable surface reconstructions for pure unstrained GaSb at typical growth conditions. However, under very Sb rich conditions a third reconstruction is experimentally observed, either a $c(2 \times 10)$ or $c(2 \times 5)$ reconstruction [32]. There is little consensus on the atomistic details of the $c(2 \times 10)/c(2 \times 5)$ reconstruction, and recent X-ray experiments rule out all of the proposed structures [32]. For this reason, we have used the $c(4 \times 4)$ reconstruction as a proxy for the $c(2 \times 5)/c(2 \times 10)$ reconstruction in our energy calculations. This substitution was chosen because the $c(4 \times 4)$ is reported in the AlSb system [31], which has the same surface reconstructions as GaSb under most growth conditions. Our DFT calculations show that the $c(4 \times 4)$ is stable

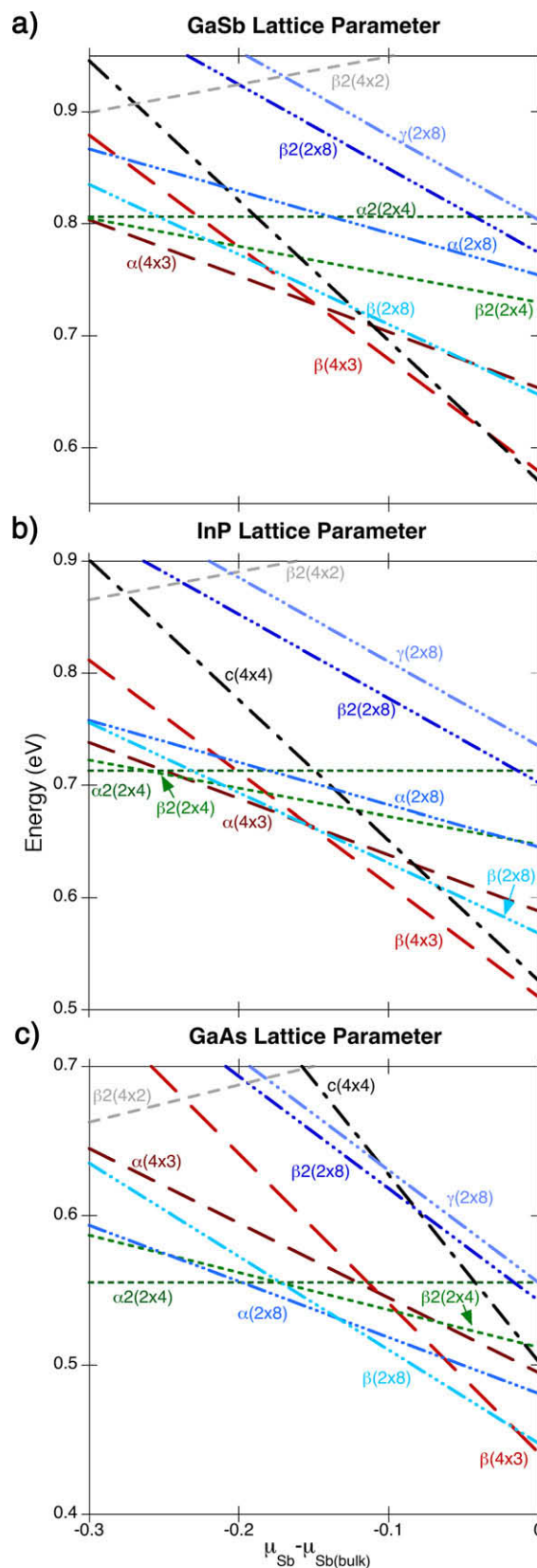


Fig. 3. Energy vs. $\mu_{\text{Sb}} - \mu_{\text{Sb(bulk)}}$ at the (a) GaSb, (b) InP, and (c) GaAs lattice parameters, respectively. The lowest line on any graph is the stable reconstruction at that chemical potential. (For interpretation of the references to colors in this figure, the reader is referred to the web version of this paper.)

only at the highest values of μ_{Sb} at the GaSb lattice parameter, consistent with expectations.

When the lattice parameter is constrained to the smaller InP lattice parameter, the relative stability of the different surface reconstructions changes as each surface atomic configuration accommodates the compressive strain differently. At the InP lattice parameter, the stable reconstructions with increasing μ_{Sb} are the $\alpha(2 \times 4)$, $\beta(2 \times 4)$, $\alpha(4 \times 3)$ and $\beta(4 \times 3)$. The $c(4 \times 4)$ proxy has increased in energy such that it is no longer stable at any chemical potential. The $\alpha(4 \times 3)$ and $\beta(4 \times 3)$ remain stable, however, not over as large a chemical potential range. The $\beta(2 \times 8)$ reconstruction decreases in energy relative to the (4×3) reconstructions and approaches stability at the intersection of the $\alpha(4 \times 3)$ and $\beta(4 \times 3)$ lines.

This shift in stability of the various surface reconstructions continues as the lattice parameter is further reduced to that of GaAs (Fig. 3c) where the stable reconstructions with increasing Sb are the $\alpha(2 \times 4)$, $\alpha(2 \times 8)$, $\beta(2 \times 8)$, and $\beta(4 \times 3)$ reconstructions. The DFT results show the stability of the (4×3) reconstructions is all but eliminated with the $\beta(4 \times 3)$ stable only at very high values of μ_{Sb} , and the (2×4) and (2×8) reconstructions are the stable reconstructions at most chemical potentials. This agrees with experimental results which demonstrate the stability of the (2×4) , (2×8) and (4×3) [18,19,22,23,31,33].

At the GaAs lattice parameter, it is evident that the stable GaSb/GaAs- (2×8) reconstruction is the $\alpha(2 \times 8)$ or $\beta(2 \times 8)$. Interestingly, the $\beta(2 \times 8)$ has a lower energy than the $\alpha(2 \times 8)$ at the InP lattice parameter, but the $\alpha(2 \times 8)$ decreases much more rapidly in energy as the lattice constant is reduced further to become stable at the GaAs lattice parameter. This may be due to the highly tensile cation–cation bond present in this structure. Thus, as the lattice parameter is reduced, the amount of strain within this cation–cation bond is reduced, dramatically lowering the energy of the structure. The low energy of the $\alpha(2 \times 8)$ and $\beta(2 \times 8)$ reconstructions relative to other reconstructions may be due to the presence of surface Sb dimers in both the $[1\ 1\ 0]$ and $[1\ \bar{1}\ 0]$ directions, which may allow the 7% mismatch strain of the surface to be relieved along both directions.

These results also show that the proposed $\beta(2 \times 8)$ and $\gamma(2 \times 8)$ reconstructions are never in thermodynamic equilibrium, as they are always >25 meV per unit area higher than the stable reconstruction at any μ_{Sb} at any lattice parameter. The $\gamma(2 \times 8)$ is always greater in energy than the $\beta(2 \times 8)$, which is consistent with III-As calculations that show the $\beta(2 \times 4)$ higher in energy than the $\beta(2 \times 8)$ reconstruction. The higher energies of the $\beta(2 \times 4)$ and $\gamma(2 \times 8)$ reconstructions are likely due to the Sb anti-sites in these structures. Experimentally, it is possible that anti-sites may form given that both Sb and Ga are required but only Sb is supplied in the growth flux. Despite this, our results suggest that no anti-sites form in these experiments as the STM results are consistent only with the $\alpha(2 \times 8)$ and $\beta(2 \times 8)$ which show no intensity change along the dimer chains in the $[1\ \bar{1}\ 0]$ direction.

4. Conclusions

These DFT calculations show that the $\alpha(2 \times 8)$ and $\beta(2 \times 8)$ are the stable reconstructions of thin layers of GaSb at the GaAs lattice parameter, in agreement with the experimental STM images. The $\beta(2 \times 8)$ and $\gamma(2 \times 8)$ are never stabilized due to the high energy of the anti-site defect. The low energy of the $\alpha(2 \times 8)$ and $\beta(2 \times 8)$

reconstructions relative to other reconstructions may be due to the presence of Sb dimers oriented perpendicularly which may relieve the 7% lattice mismatch strain more thoroughly. These reconstructions are easily formed from the GaAs buffer layer (2×4) reconstruction of the underlying GaAs buffer layer by simply filling in the trench between two adjacent cells with two cations and eight anions, suggesting an easy kinetic pathway by which to form these reconstructions.

Acknowledgements

The authors would like to thank Diana Huffaker for insight into the GaSb/GaAs system, and Chris Pearson for his expertise in STM data analysis. This work was performed in part at the US Department of Energy, Center for Integrated Nanotechnologies, at Los Alamos National Laboratory (Contract DE-AC52-06NA25396) and Sandia National Laboratories (Contract DE-AC04-94AL85000).

References

- [1] S. Froyen, A. Zunger, Phys. Rev. B 53 (1996) 4570.
- [2] G.A. Somorjai, Annu. Rev. Phys. Chem. 45 (1994) 721.
- [3] G. Zhou, J.C. Yang, J. Mater. Res. 20 (2005) 1684.
- [4] B. Voigtländer, Surf. Sci. Rep. 43 (2001) 127.
- [5] U. Welp, V.K. Vlasov, X. Liu, J.K. Furdyna, T. Wojtowicz, Phys. Rev. Lett. 90 (2003) 167206.
- [6] M.D. Pashley, Phys. Rev. B 40 (1989) 10481.
- [7] V. Bresslerhill, M. Wassermeier, K. Pond, R. Maboudian, G.A.D. Briggs, P.M. Petroff, W.H. Weinberg, J. Vac. Sci. Technol. B 10 (1992) 1992.
- [8] A.S. Bracker, M.J. Yang, B.R. Bennett, J.C. Culbertson, W.J. Moore, J. Cryst. Growth 220 (2000) 1492.
- [9] J.E. Bickel, N.A. Modine, C. Pearson, J. Mirecki Millunchick, Phys. Rev. B 77 (2008) 125308.
- [10] C. Ratsch, Phys. Rev. B 63 (2001) 161306.
- [11] B. Voigtländer, M. Kästner, Phys. Rev. B 60 (1999) R5121.
- [12] J.E. Bickel, A. Van der Ven, J. Mirecki Millunchick, N.A. Modine, Appl. Phys. Lett. 92 (2008) 062104.
- [13] J.H. Cho, S.B. Zhang, A. Zunger, Phys. Rev. Lett. 84 (2000) 3654.
- [14] Malik, van der Ziel, J. Appl. Phys. 59 (1968) 3909.
- [15] G. Balakrishnan, J. Tatebayashi, A. Khoshakhlagh, S.H. Huang, A. Jallipalli, L.R. Dawson, D.L. Huffaker, Appl. Phys. Lett. 89 (2006) 161104.
- [16] S.H. Huang, G. Balakrishnan, A. Khoshakhlagh, A. Jallipalli, L.R. Dawson, D.L. Huffaker, Appl. Phys. Lett. 88 (2006) 131911.
- [17] J. Tatebayashi, A. Khoshakhlagh, S.H. Huang, L.R. Dawson, G. Balakrishnan, D.L. Huffaker, Appl. Phys. Lett. 89 (2006) 203116.
- [18] F. Maeda, Y. Watanabe, M. Oshima, Phys. Rev. B 48 (1999) 14733.
- [19] P. Moriarty, P.H. Beton, Y.R. Ma, M. Henini, Phys. Rev. B 53 (1996) R16148.
- [20] W.G. Schmidt, F. Bechstedt, Phys. Rev. B 55 (1997) 13051.
- [21] N. Esser, A. Shkrebtii, U. Resch-Esser, C. Springer, W. Richter, W. Schmit, F. Bechstedt, R.D. Sole, Phys. Rev. Lett. 77 (1996) 4402.
- [22] L.J. Whitman, B.R. Bennett, E.M. Kneedler, B.T. Jonker, B.V. Shanabrook, Surf. Sci. Lett. 436 (1999) L707.
- [23] P. Laukkanen, R.E. Perala, R.-L. Vaara, I.J. Vayrynen, M. Kuzmin, J. Sadowski, Phys. Rev. B 69 (2004) 205323.
- [24] J.E. Bickel, C. Pearson, J. Mirecki Millunchick, Surf. Sci. 603 (2009) 14.
- [25] Y.Q. Wang, Z.L. Wang, T. Brown, A. Brown, G. May, J. Cryst. Growth 242 (2002) 5.
- [26] W. Barvosa-Carter, F. Grosse, J.H.G. Owen, J.J. Zinck, Mater. Res. Soc. Symp. Proc. 692 (2002) H8.4.1.
- [27] J. Tersoff, D.R. Hamann, Phys. Rev. B 50 (1983) 1998.
- [28] H. Yamaguchi, Y. Horikoshi, Phys. Rev. B 51 (1995) 9836.
- [29] R.R. Wixom, N. Modine, G. Stringfellow, Phys. Rev. B 16 (2003) 115309.
- [30] K. Yamaguchi, Y. Takeda, K. Kameda, K. Itagaki, Mater. Trans. 35 (1994) 596.
- [31] W. Barvosa-Carter, A.S. Bracker, J.C. Culbertson, B.Z. Nosh, B.V. Shanabrook, L.J. Whitman, H. Kim, N.A. Modine, E. Kaxiras, Phys. Rev. Lett. 84 (2000) 4649.
- [32] B.P. Tinkham, O. Romanyuk, W. Braun, K.H. Ploog, F. Grosse, M. Takahashi, T. Kaizu, J. Mizuki, J. Electron. Mater. 37 (2008) 1793.
- [33] J.J. Zinck, E.J. Tarsa, B. Brar, J.S. Speck, J. Appl. Phys. 82 (1997) 6067.